Biophysical Insights from Temperature-Dependent Single-Molecule Förster Resonance Energy Transfer

Erik D. Holmstrom and David J. Nesbitt

JILA, National Institute of Standards and Technology, University of Colorado, Boulder, Colorado 80309; email: djn@jila.colorado.edu

Department of Chemistry and Biochemistry, University of Colorado, Boulder, Colorado 80309; email: djn@jila.colorado.edu

Annu. Rev. Phys. Chem. 2016. 67:441–65

The *Annual Review of Physical Chemistry* is online at physchem.annualreviews.org

This article's doi: 10.1146/annurev-physchem-040215-112544

Keywords

nucleic acid folding, single molecule kinetics, thermodynamics, transition state theory

Abstract

Single-molecule fluorescence microscopy techniques can be used in combination with micrometer length-scale temperature control and Förster resonance energy transfer (FRET) in order to gain detailed information about fundamental biophysical phenomena. In particular, this combination of techniques has helped foster the development of remarkable quantitative tools for studying both time- and temperature-dependent structural kinetics of biopolymers. Over the past decade, multiple research efforts have successfully incorporated precise spatial and temporal control of temperature into single-molecule FRET (smFRET)-based experiments, which have uncovered critical thermodynamic information on a wide range of biological systems such as conformational dynamics of nucleic acids. This review provides an overview of various temperature-dependent smFRET approaches from our laboratory and others, highlighting efforts in which such methods have been successfully applied to studies of single-molecule nucleic acid folding.

1. INTRODUCTION

The first laser-based microscopy/spectroscopy of species at the single-molecule level was performed nearly three decades ago (1, 2). With these groundbreaking studies, an entire field of science, and indeed a completely new way of thinking, has emerged (3). The ability to probe individual molecules arguably represents the ultimate limit in analytical sensitivity. Specifically, it has allowed the physical chemistry community to challenge and explore many conventional (albeit, on closer inspection, often flawed) assumptions—for example, sample homogeneity (i.e., all covalently identical molecules behave identically) and kinetic synchronization (i.e., each molecular transformation experiences the same zero of time)—implicit in ensemble experiments that can only observe the population-averaged behavior of a sample (4). Soon after these pioneering observations of single molecules, well-established concepts from Förster resonance energy transfer (FRET) (5) were applied to individual molecules in order (6) to monitor the distance-dependent efficiency of energy transfer (E_{FRET}; Equation 1) between spectrally overlapping molecular dipoles (e.g., fluorophores) with a characteristic Förster distance (R_0):

$$E_{\mathrm{FRET}}(r) = \frac{R_0^6}{r^6 + R_0^6}. \tag{1}$$

Such single-molecule FRET (smFRET) observations unambiguously demonstrated that the combination of these techniques could be used as a powerful and elegant spectroscopic ruler (7, 8), capable of measuring nanometer-scale dynamics with high temporal resolution. Perhaps the most influential applications were to studies of biological polymers (e.g., proteins, DNA, and RNA; 9–11) because (*a*) the dimensions of these molecules are commensurate with the R_0 values associated with commonly used donor-acceptor FRET pairs ($R_0 \approx 3$–7 nm) and (*b*) these biopolymers are sufficiently large (>10 kDa) that the presence of small spectroscopic probes (<1 kDa) can be expected to have relatively negligible effects on conformational folding dynamics. Ever since the first smFRET investigations of biopolymers, this microscopy technique has been an extremely informative tool for the molecular biophysics community (12). Indeed, multiple reviews in the past decade have highlighted prominent advances in biology and biochemistry resulting from smFRET-based studies (13–16); these advances serve as an enduring testament to the power and importance of these methods. Over this time period, many of the initial challenges associated with smFRET techniques have been overcome or greatly reduced, allowing researchers to further push the boundaries of this experimental technique (17, 18). One particularly noteworthy advance has been the coupling of smFRET experiments with precise control of external physical parameters such as temperature.

The control of temperature in experiments at the single-molecule level represents a rather simple and straightforward contribution; it has nevertheless proved to be enormously powerful in that it enables researchers to approach biological problems with the more quantitative perspective of a physical chemist. The temperature dependence of chemical, biochemical, and biological phenomena studied via smFRET, which serves as the central unifying theme of this review, is an informative physical property related to chemical reaction rates and equilibrium constants (K_{eq}) based on time-honored and well-established thermodynamic principles. Arguably the most powerful of these principles is the thermodynamic expression

$$\Delta G^{\circ} = -RT\ \ln[K_{\mathrm{eq}}] = \Delta H^{\circ} - T\Delta S^{\circ}, \tag{2}$$

which relates the temperature dependence of K_{eq} to the enthalpic (ΔH^{o}) and entropic (ΔS^{o}) difference between the products and reactants under standard state conditions, where ΔG^{o} is the change in free energy and T is absolute temperature in Kelvin. Furthermore, this equation can be used to partition free energy folding landscapes (19) into their entropic and enthalpic

components, fundamentally enhancing our understanding of biomolecular structural dynamics and permitting the development of thermodynamically motivated mechanisms to describe the underlying chemical processes. Most importantly, such thermodynamic information provides us with greatly improved physical models with which to predict the temperature dependence of the biological process of interest. Although these insights can be quite revealing when obtained at the ensemble level, they can be even more illustrative when they originate from single-molecule experiments that lack the complicating assumptions implicit in ensemble experiments.

Sections 2 and 3 of this review each simultaneously address two separate but conceptually related components of temperature-dependent smFRET: (*a*) the methodological aspects of temperature control and (*b*) the application of these methods to various biophysical problems. In Section 2, we first briefly review one of the more common methodological approaches to temperature-dependent smFRET experiments, referred to as stage-based heating. This section includes a short practical description of this heating technique, as well as a survey of several applications of stage-based heating methods to biophysical studies of conformational transitions in nucleic acids. Section 3 then explains a more advanced approach to control the experimental temperature of an smFRET sample called laser-based heating. This is followed by a summary of how such techniques have been exploited to study biophysical systems with more demanding thermal constraints. In Section 4, many of the ongoing experimental challenges and difficulties associated with temperature-dependent smFRET are discussed, along with a few brief indications of potential solutions. As a whole, this review aims to present a comprehensive and informative survey of temperature-dependent FRET and the biophysical insights that it has helped produced.

2. STAGE-BASED HEATING

Many of the first attempts to bring temperature control to single-molecule samples relied simply on heating large objects associated with the various components of a fluorescence microscope. In perhaps the most common implementation of the technique, a simple, stage-based heater is used to control the temperature of the microscope stage and/or sample holder (20, 21) (for alternative implementations of stage-based heating, see the sidebar Alternative Stage-Based Heating Techniques). This dictates the temperature of the medium containing the molecules of interest

ALTERNATIVE STAGE-BASED HEATING TECHNIQUES

In certain cases, geometric constraints of the microscope can restrict the use of stage-based devices, rendering them ineffective sources of temperature control. However, even under such conditions, at least two possible alternative approaches exist for stage-based heating. The first is to increase the size of the heated volume, i.e., warm the entire microscope system within a temperature- and humidity-controlled enclosure, as is occasionally done in the field of live cell imaging. Such strategies are problematic, however, as repeated expansion and contraction caused by unavoidable temperature changes can lead to instabilities in optical alignment, resulting in decreased performance of the microscope system. The second option is to avoid geometric constraints associated with stage-based heating devices by dramatically decreasing the size of the heated volume. This approach has proven successful via the development and production of temperature-controlled microfluidic devices designed for both confocal (75) and TIRF (46, 102) smFRET microscopes. Additionally, it is worth mentioning that a recent report describes how a commercially available real-time single-molecule sequencing instrument (Pacific Biosciences of California) can be modified for precise, multicolor smFRET measurements at various temperatures (103), providing yet another possible alternative.

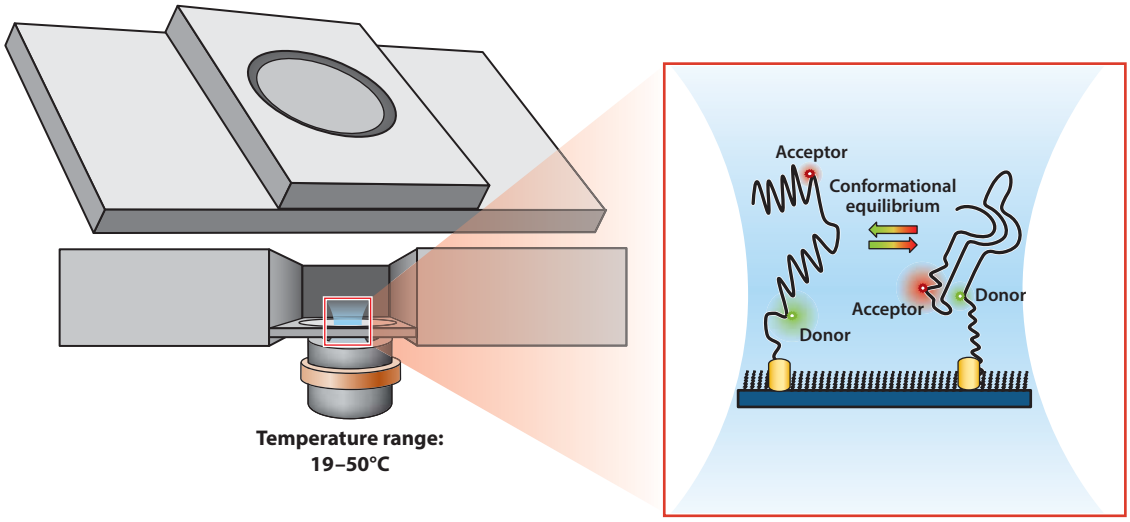

Figure 1

Schematic illustration of a common stage-based heating device and a microscope objective equipped with a thermal collar. The temperature-controlled chamber, containing the sample of interest, rests on the microscope stage (not shown, for clarity) directly above the objective. The heated objective collar minimizes any potential thermal gradients within the sample, resulting in a nearly uniform spatial temperature profile.

(**Figure 1**). These commercially available devices and their custom-built counterparts provide a rather robust method to control sample temperatures for a wide variety of microscope systems (22, 23). Such devices frequently offer plug-and-play operation and rarely require advanced software packages or sophisticated procedures for installation. Additionally, a thermal objective collar can be used to control the temperature of the microscope objective, thus minimizing the potential for any thermal gradients between the temperature-controlled sample and the otherwise thermally conductive microscope objective (20, 21).

One of the crucial advantages of stage-based heating techniques is that the steady-state temperature of the system can be accurately determined using a well-calibrated thermocouple or thermistor. Another advantage, at least for the less sophisticated plug-and-play systems, is that they can quickly and easily be incorporated into existing smFRET microscope systems with minimal effort (20, 21). Together, these two benefits contribute to the predominance of stage-based heating techniques for temperature-dependent smFRET measurements.

2.1. Conceptual Framework

The conceptual foundation for temperature-dependent smFRET is quite simple and builds on the fundamental physical chemistry topics of kinetics and thermodynamics. For smFRET studies using total internal reflection fluorescence (TIRF) or confocal fluorescence microscopy, one common representation of the experimental data is a so-called single-molecule fluorescence time trajectory (12, 24, 25), which is simply a plot of the donor and acceptor signals as a function of time (**Figure 2*a***) for an individual surface-immobilized molecule (**Figure 2*b***). Such a fluorescence time trajectory can readily be converted into an E_{FRET} time trajectory (**Figure 2*c***) by simply taking the ratio of the acceptor signal to the sum of the donor and acceptor signals (Equation 3), after correcting for factors such as quantum yield and optical filter transmission that influence γ, the ratio of detection

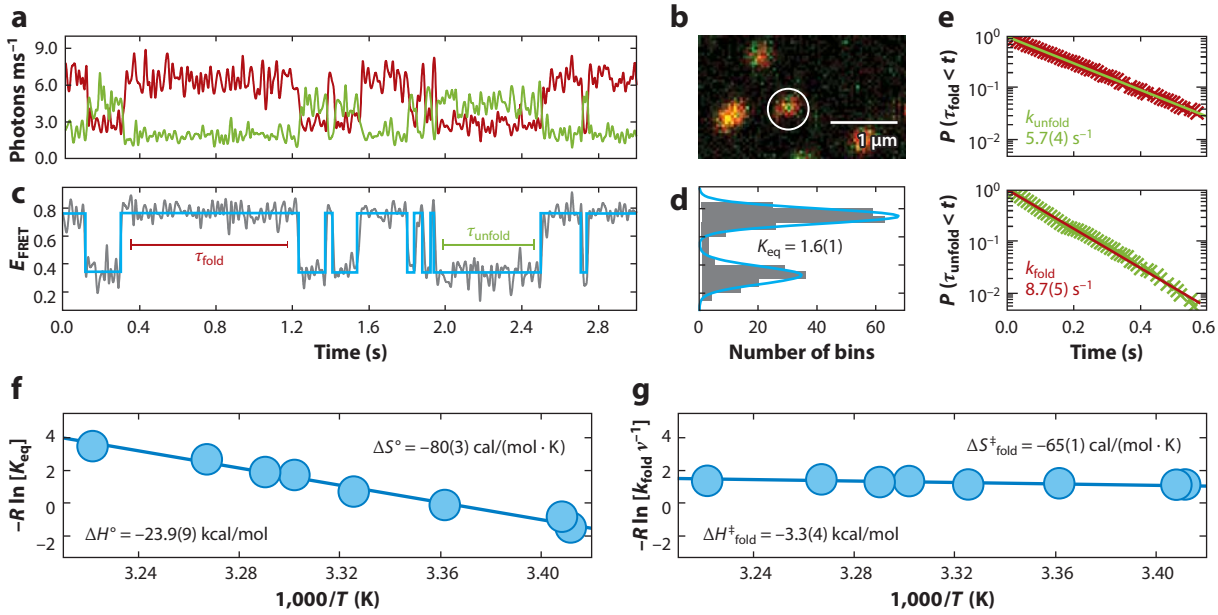

Figure 2

Conceptual framework for temperature-dependent smFRET. (*a*) Representative donor (*green*) and acceptor (*red*) fluorescence time trajectories from a surface-immobilized molecule. (*b*) Red-green, false-color surface representation of diffraction-limited features associated with immobilized molecules. (*c*) Representative FRET efficiency (E_{FRET}) time trajectory (*gray*), with the corresponding two-state hidden Markov maximum likelihood trajectory (*light blue*). (*d*) Time-averaged histogram of E_{FRET} values from panel *c*, nicely demonstrating the two-state behavior and the associated equilibrium constant (K_{eq}). (*e*) Log-linear dwell-time probability plots for folded (*top*) and unfolded (*bottom*) dwell times. Solid lines correspond to single-exponential fits used to determine the respective rate constants. (*f*) Van't Hoff plot depicting the standard-state entropic ($\Delta S°$) and enthalpic ($\Delta H°$) change associated with the conformational equilibrium. (*g*) Eyring plot depicting the entropic and enthalpic components of the free energy barrier for the folding process. The data used to generate this figure are associated with previously published work (31).

efficiencies for each of the two detection channels:

$$E_{FRET}(r) = \frac{S_{acceptor}}{S_{acceptor} + \gamma S_{donor}}. \quad (3)$$

As a result of the distance dependence of FRET (Equation 1), any stochastic shift in the dye-dye distance resulting from a conformational fluctuation of the biomolecule can be read out as either an anticorrelated change in donor and acceptor fluorescence (**Figure 2*a***) or a change in E_{FRET} (**Figure 2*c***). For well-resolved, two-state E_{FRET} time trajectories (e.g., **Figure 2*c***), a simple threshold-based algorithm (26) can be used to identify the time points associated with each and every threshold crossing. These time points are used to determine the duration spent in a given conformation before undergoing a transition (τ_{dwell}). For the analysis of more complex smFRET time trajectories, (27) alternative approaches (28–30) take clever advantage of various statistical methods that use the Viterbi algorithm and hidden Markov modeling to determine transitions between states (**Figure 2*c***), and in some cases the underlying kinetic rate constants. After having determined the dwell times, researchers can calculate the time-dependent probability of observing a dwell time longer than time t, represented as a plot of $P(\tau_{dwell} > t)$ versus t (**Figure 2*e***). This plot provides information about the underlying conformational kinetics. Sufficient sampling of such plots typically requires hundreds to thousands of individual τ_{dwell} measurements, at which point

the resulting distributions become experimentally indistinguishable. For a simple unimolecular process (e.g., folded → unfolded), such a distribution of dwell times will decay exponentially, with characteristic time constants that describe the rate constants associated with the observed conformational transitions (**Figure 2*e***). As a rigorous check of internal consistency, time-averaged E_{FRET} histograms (**Figure 2*d***) can be constructed from the corresponding time trajectory to determine the relative occupancy of the two conformations (i.e., K_{eq}), which should be identical to the appropriate ratio of the rate constants (**Figure 2*e***). As a consequence, these powerful surface-immobilized smFRET-based approaches allow for the determination of both (*a*) the equilibrium constant and (*b*) forward/backward rate constants for a conformational transition of interest.

With the assistance of smFRET sample heating techniques (**Figure 1**), the temperature dependence of these physical parameters can also be explored, enabling thermodynamic measurements of single molecules. The conceptually simple, surface-immobilized smFRET experiments, highlighted above, can be performed over a range of experimental temperatures to evaluate the temperature dependence of rate and equilibrium constants. Using the temperature-dependent equilibrium constant data, ΔG° can be partitioned into ΔH° and ΔS° via mathematical rearrangement of Equation 2 to yield

$$-R\ \ln[K_{eq}] = \Delta H^\circ \left[\frac{1}{T}\right] - \Delta S^\circ. \tag{4}$$

This expression facilitates a so-called Van't Hoff analysis (**Figure 2*f***), whereby a plot of $-R\ \ln[K_{eq}]$ versus $[1/T]$ yields a slope that represents the standard-state enthalpy change for the conformational equilibrium (ΔH°) and an intercept that represents the corresponding standard-state entropy change ($-\Delta S^\circ$).

Similarly, various formulations of transition state theory can be used to interpret the temperature dependence of the rate constants, which permits determination of the enthalpic and, in certain cases, entropic components of the free energy barrier associated with the observed conformational transitions (**Figure 2*g***). For example, a variation of activated complex theory (ACT) (31) can be used to derive an expression, similar in form to the above Van't Hoff equation (Equation 4), that describes the thermodynamic relationship between the rate constant, k, and temperature, T (Equation 5):

$$-R\ \ln[k\nu^{-1}] = \Delta H^\ddagger \left[\frac{1}{T}\right] - \Delta S^\ddagger. \tag{5}$$

In this so-called Eyring equation, $\Delta H^\ddagger$ is the enthalpy change and $\Delta S^\ddagger$ is the entropy change required to reach the transition state, and ν represents the vibrational attempt frequency associated with moving from a conformation contained within a local free-energy minimum toward the transition state barrier. The experimental approaches and physicochemical concepts highlighted above form some of the main conceptual pillars of temperature-dependent smFRET. In recent years, these ideas have been successfully applied to perform thermodynamic measurements at the single-molecule level in several biomolecular systems, particularly those involving nucleic acids.

2.2. Nucleic Acid Studies

For many decades, temperature has been an extremely useful variable for ensemble studies of nucleic acid thermodynamics (32–34). For example, spectroscopic thermal denaturation experiments have been a major workhorse in many biophysical studies of nucleic acid structure formation (35–37), including those studies responsible for generating the thermodynamic parameters (38) associated with nucleic acid secondary structure prediction algorithms (39, 40). It is a natural progression to extend these temperature-dependent ideas to smFRET experiments, thereby

eliminating numerous assumptions implicitly associated with ensemble studies. Almost 15 years ago, while smFRET techniques were still in their infancy, some of the original demonstrations of the spectroscopic technique used temperature as a controlled variable (41). These seminal experiments demonstrated for the first time the feasibility of such single-molecule DNA hairpin melting experiments. Since then, many researchers have combined stage-based heating and smFRET to gain valuable thermodynamic insights related to both secondary and tertiary conformational transitions in a diverse array of DNAs [e.g., hairpins (41), duplexes (42), G-quartets (43)], RNAs [e.g., *Tetrahymena* ribozymes (44), four-way junctions (45), human telomerase RNA pseudoknots (43)], and even ribonucleoproteins, such as the ribosome (46). Temperature-dependent smFRET studies have also been used to explore the thermodynamic influences of various cosolutes on these types of conformational transitions. What follows is a summary of a few instances in which such stage-based heating techniques have been successfully applied to biophysical studies of nucleic acid conformational dynamics.

2.2.1. Duplex hybridization. The bimolecular association of two complementary strands of DNA is arguably one of the most important biochemical reactions for life on earth. Knowledge of the stability of duplex DNA, determined via ensemble thermal denaturation, has helped facilitate some of the most significant advancements of the twentieth century, including various polymerase chain reaction–based biotechnologies. Despite these efforts, a predictive understanding of the temperature-dependent kinetics for such hybridization processes remains elusive. Temperature-dependent smFRET-based experimental techniques can offer unique and valuable perspectives on this problem. By way of demonstration, our group has recently explored the thermally induced melting of an 8-bp double-stranded DNA duplex using confocal fluorescence microscopy and stage-based heating methods (42). In these experiments, the duplex association and dissociation rate constants (k_{on} and k_{off}, respectively) are determined from single-molecule time trajectories that display discrete events where FRET occurs between a donor fluorophore attached to a surface-immobilized single-stranded DNA and the acceptor of an otherwise freely diffusing complementary oligonucleotide (**Figure 3*a***). The close proximity of the two fluorophores in the duplex results in a high E_{FRET}, whereas the absence of a complementary strand corresponds to the lack of a proximal acceptor and therefore no energy transfer. This bimolecular association-dissociation equilibrium allows one to examine the underlying thermodynamics by observing the effect of temperature on both the rate constants and the equilibrium constant ($K_{eq} = k_{on}/k_{off}$) for DNA duplex association (**Figure 3*b–d***). As expected, heating destabilizes the duplexes and therefore decreases the equilibrium constant. A Van't Hoff analysis of single-molecule K_{eq} values (**Figure 3*b***) reveals consistently negative slopes with positive intercepts, which implies that both $\Delta H^\circ < 0$ and $\Delta S^\circ < 0$ for the association equilibrium over a wide range of monovalent conditions. This behavior is to be expected (for a discussion of instances where this behavior is not observed, see the sidebar Endothermic Nucleic Acid Conformational Transitions): The exothermic release of heat results from base stacking and hydrogen bond formation, and the decrease in entropy results from reduced conformational flexibility in the duplex structure.

Much of the above equilibrium thermodynamic analysis could have been obtained from ensemble studies. However, the critical additional power of single-molecule methods is that, unlike in ensemble conditions, discrete conformational transitions in individual molecules can readily be detected, even for a system nominally at equilibrium. The frequency of these events provides information that can be used to determine the kinetic origin of an equilibrium effect. For example, it is well known that temperature destabilizes duplex DNA. However, we can see from single-molecule DNA duplex association-dissociation experiments that k_{off} increases rapidly with increasing temperature, whereas k_{on} is nearly independent of temperature. Therefore, these smFRET

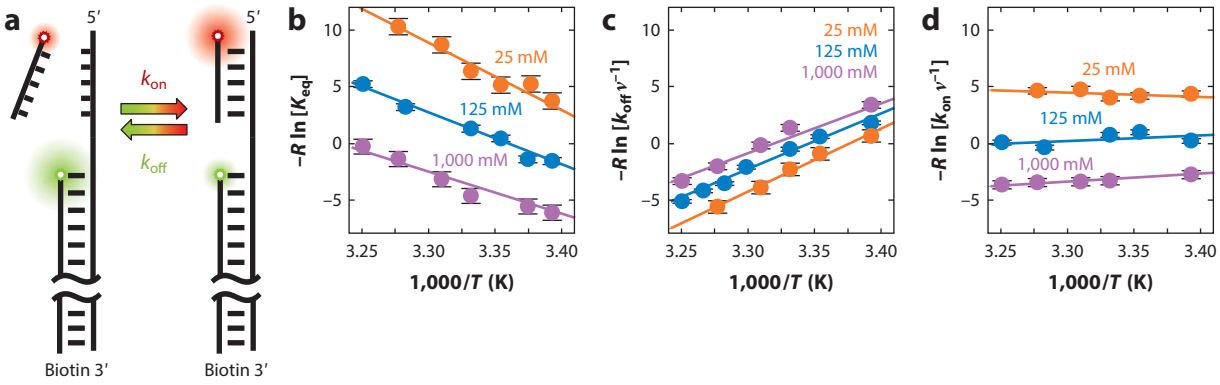

Figure 3

DNA duplex hybridization. (*a*) Schematic representation of the smFRET DNA construct used to study the thermodynamics of duplex association and dissociation as a function of [NaCl]. (*b*) Van't Hoff plot showing the enthalpic (*slope*) and entropic (*intercept*) components of the free energy difference for duplex association. Increasing [NaCl] results in a strong entropic offset. Eyring plots for the (*c*) association and (*d*) dissociation rate constants, which reveal that the [NaCl]-dependent entropic offset in panel *b* arises primarily from the association rate constant (k_{on}). The data used to generate this figure are associated with previously published studies (42) from our group.

studies convincingly demonstrate that the kinetic origin of thermal denaturation is a temperature-dependent increase in k_{off}.

This can be better quantified in the context of ACT (Equation 5), which predicts that an Eyring plot of $-R \ln[k\nu^{-1}]$ versus $[1/T]$ should yield a straight line with a slope of $\Delta H^{\ddagger}$ and an intercept of $-\Delta S^{\ddagger}$, as depicted in **Figure 3*c*,*d***, which shows the temperature dependence of k_{off} and k_{on} across a series of salt concentrations. The accessibility of both temperature-dependent equilibrium information and kinetic information for the same nucleic acid constructs under various experimental conditions is particularly revealing. For example, the dissociation rate constant for a near-physiological ionic strength (e.g., 125 mM NaCl) has an enthalpic barrier of $\Delta H^{\ddagger}_{off} =$ 45(3) kcal/mol, which is experimentally indistinguishable from the overall enthalpy change associated with a dissociation event [$\Delta H°_{off} = 46(2)$ kcal/mol]. This observation, along with a demonstrably weak temperature dependence of k_{on} (**Figure 3*d***), indicates that formation of the DNA duplex must have a negligible enthalpic activation barrier.

ENDOTHERMIC NUCLEIC ACID CONFORMATIONAL TRANSITIONS

Owing to the formation of hydrogen bonds and base stacking interactions, one might assume that all nucleic acid conformational transitions would be exothermic, but this is not the case. One important counterexample includes a conformational transition associated with the folding pathway of the *Tetrahymena* ribozyme; specifically, this example involves docking of the P1 helix into the core of the ribozyme. Temperature-dependent smFRET techniques from the Herschlag group (44) used to study conformational dynamics of the P1 helix have revealed a folding equilibrium constant that increases with increasing temperature. This pronounced endothermicity (i.e., $\Delta H° > 0$) results from two rate processes that are differentially thermally activated ($\Delta H^{\ddagger}_{dock} > \Delta H^{\ddagger}_{undock} > 0$). With the assistance of additional biochemical and biophysical studies, the authors have attributed this endothermicity to the presence of a stable, nonnative interaction (called a kinetic trap) in the undocked conformation. This interaction must be broken prior to forming the transition state and is more enthalpically stable than the native interaction.

One surprising result of this study is that increasing [NaCl] promotes duplex formation primarily via an entropically driven increase in the association rate constant, resulting in flat and parallel lines at three different salt concentrations (**Figure 3*d***), which are vertically offset from one another. The thermodynamic origin of this effect can be attributed to a salt-induced ordering of the individual single strands [a theory previously proposed to explain the results of ensemble thermodynamic studies (47)], resulting in so-called stacked conformations that are structurally primed for duplex association. At elevated salt concentrations, the newly acquired order in the single-stranded DNAs reduces the entropic component of the free energy barrier, resulting in an increase in k_{on} and therefore net stabilization of the associated complex. These studies of a conceptually simple biophysical problem nicely demonstrate how thermally induced conformational transitions in nucleic acids can be investigated using temperature-dependent smFRET techniques and how results from these studies can be used to reconstruct the enthalpic and entropic components of the free energy landscape.

2.2.2. GAAA tetraloop-tetraloop receptor. One of the best-studied classes of tertiary interactions in nucleic acids is that of GNRA tetraloops with their associated receptors (48). Within this ubiquitous class of tertiary interactions, the GAAA tetraloop-tetraloop receptor from the *Tetrahymena* ribozyme has been the subject of extensive biochemical and biophysical investigations, including numerous temperature-dependent smFRET studies. In a collection of works from our group, three synthetic oligonucleotides have been used to construct an isolated variant of this tertiary motif that contains a biotin moiety for surface immobilization and a Cy3-Cy5 donor-acceptor pair for FRET (**Figure 4*a***). Temperature-dependent studies of this FRET-labeled GAAA tetraloop-tetraloop receptor have nicely revealed that the enthalpy of formation ($\Delta H°$) associated with this tertiary interaction is strongly negative (i.e., exothermic) (21) (for a discussion of instances where this behavior is not observed, see the sidebar Endothermic Nucleic Acid Conformational Transitions).

Our group has uncovered new kinetic information regarding this GAAA tetraloop-tetraloop receptor tertiary interaction using single-molecule temperature-dependent kinetic, rather than equilibrium, studies (**Figure 4*a***). Careful inspection of the dwell times associated with E_{FRET} trajectories (**Figure 4*b***) shows that the folded event durations are shorter at elevated temperatures, whereas the unfolded dwell times are largely temperature-independent. This demonstrates (**Figure 4*c***) that the folding rate constant (k_{fold}) for this tertiary docking event is much less temperature-dependent than the unfolding rate constant (k_{unfold}) (49). This thermally accelerated unfolding shifts the equilibrium toward the low-E_{FRET} population (**Figure 4*b***). Similar to what was described in Section 2.2.1, the absence of a temperature-dependent folding rate constant reflects the small enthalpic transition state barrier ($\Delta H^{\ddagger}_{fold} \approx 0$ kcal/mol) for the folding process.

Indeed, as a result of experimental access to both temperature-dependent equilibrium and kinetic studies, we can now deconstruct the overall free energy landscape into the corresponding enthalpic and entropic coordinates for both the forward and reverse processes. This is compactly summarized for the GAAA tetraloop-tetraloop receptor tertiary interaction in **Figure 4*d***, in which the left, right, and middle horizontal lines correspond to unfolded, folded, and transition state regions of the free energy landscape, respectively. These plots indicate that, for this conformational transition, the folding dynamics for accessing the transition state barrier are largely entropic in nature, whereas the unfolding dynamics are dominated by a strong enthalpic barrier. A physically motivated description of such a reaction coordinate is as follows: Folding is restricted by formation of a highly ordered compact transition state, after which point the folding process continues toward products with relatively modest changes in entropy and much more pronounced enthalpic rewards, resulting from the formation of stabilizing interactions. Stated in another way, the barrier

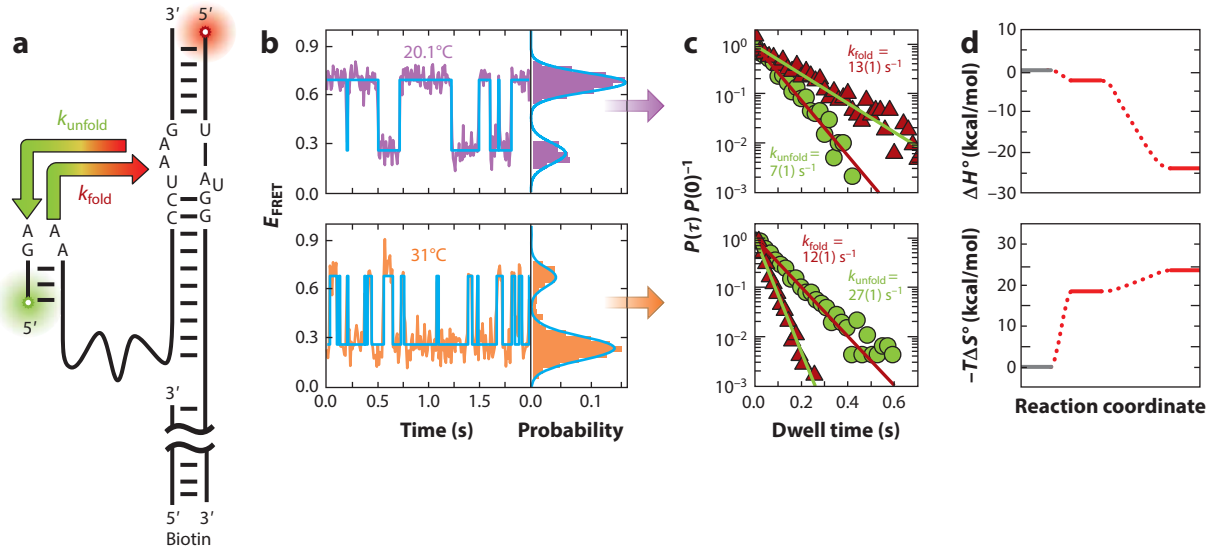

Figure 4

GAAA tetraloop-tetraloop receptor. (*a*) Schematic diagram for the smFRET RNA construct designed to isolate the ubiquitous tertiary interaction of the GAAA tetraloop and its 11-nt receptor. (*b*) Example FRET efficiency (E_{FRET}) time trajectories at two different temperatures, demonstrating that the duration of time spent in the high-E_{FRET} conformation is shorter at elevated temperatures, resulting in molecules that spend more time unfolded. (*c*) Quantitative analysis of the distribution of dwell times for the two experimental temperatures, confirming that the unfolding rate constant substantially increases with temperature, whereas the folding rate constant is largely independent of temperature. (*d*) Enthalpic ($-\Delta H°$) and entropic ($-T\Delta S°$) reaction coordinates for the formation of the GAAA tetraloop-tetraloop receptor interaction constructed using the temperature dependence of the equilibrium and rate constants. The data used to generate this figure were obtained from previously published smFRET studies (49) by our group.

to folding is early, which further supports the prevailing notion that many conformational changes in nucleic acids have transition states that are structurally dissimilar to the nucleic acids' final folded conformations (44, 50, 51). Looking toward the future, the availability of information on such enthalpic and entropic contributions to folding/unfolding processes offers additional insights into the folding landscapes of structured biomolecules, as well as quantitative benchmarks for detailed molecular dynamics simulations.

2.2.3. Nucleic Acid Cosolutes. Temperature-dependent smFRET has also been used to explore the thermodynamic influence of various cosolutes [e.g., mono- and divalent metal cations (31, 49), molecular crowding agents (52), and nonionic osmolytes (53)] on nucleic acid conformational transitions. One fascinating source of inspiration for these studies is the cellular milieu, which consists of a complex and highly concentrated amalgamation of cosolutes (e.g., metal ions, biopolymers, cofactors). We are only beginning to understand how these cosolutes, both in isolation (e.g., in vitro) and in complex mixtures (e.g., in vivo), influence the behaviors of many biomolecules. Additionally, in such highly concentrated solutions, the volume associated with dissolved solutes can account for a measurable fraction of the total solution volume, which alone can profoundly affect the energetics of such biomolecules. Given the extremely well-characterized and ubiquitous nature of the GAAA tetraloop-tetraloop receptor, this tertiary interaction serves as an excellent model system for exploring the thermodynamic effects of cosolute-influenced nucleic acid conformational transitions.

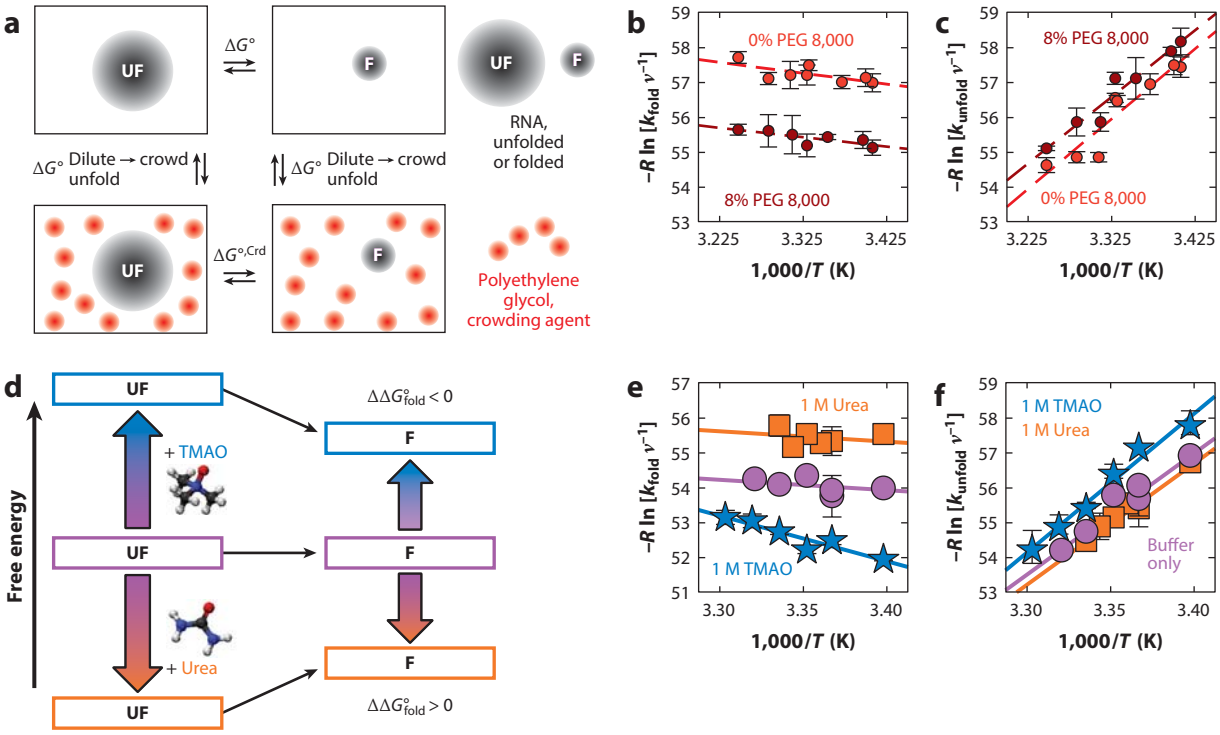

Figure 5

Cosolute-influenced conformational transitions in nucleic acids. (*a*) Thermodynamic cycle for the influence of molecular crowding on biomolecular folding. High-molecular-weight polyethylene glycol (hmwPEG) is used to vary the amount of excluded volume within the solution. (*b*,*c*) Eyring plots of the (*b*) folding and (*c*) unfolding rate constants for the GAAA tetraloop-tetraloop receptor interaction in the presence and absence of molecular crowding agents. Note the strong entropic offset associated primarily with the folding rate constant, which suggests that hmwPEG is an enthalpically inert crowding agent, making hmwPEG a suitable crowding agent for studying the effects of excluded volume. (*d*) Free energy diagram for the energetic influences of the osmolytes trimethylamine-*N*-oxide (TMAO; *blue*) and urea (*orange*). (*e*,*f*) Eyring plots of the (*e*) folding and (*f*) unfolding rate constants for the GAAA tetraloop-tetraloop receptor interaction in the presence and absence of stabilizing (TMAO) and destabilizing (urea) osmolytes. The presence of TMAO alters both the enthalpic (*slope*) and entropic (*intercept*) components of the free energy barrier to folding. This highlights a second way in which TMAO can influence nucleic acid conformational transitions—a strong, unfavorable, preferential interaction with phosphate groups, resulting in both entropic and enthalpic changes to the free energy surface, that is unlike the weak, unfavorable, preferential interaction with the nucleobases, which gives rise to predominantly entropic changes to the folding landscape. Abbreviations: F, fold; UF, unfold. The data used to generate this figure were obtained from previously published work (52, 53).

One particularly interesting class of nucleic acid cosolutes is simply biopolymers, which can occupy as much as 30% of the total solution volume within a cell (54). Such excluded volumes can restrict the conformational freedom of the molecules of interest, and thus substantially alter the energetics of folding. In a recent collection of temperature-dependent smFRET experiments from our group, the formation of the GAAA tetraloop-tetraloop receptor interaction (**Figure 4*a***) was studied in the presence of crowding agents, such as high-molecular-weight polyethylene glycol (hmwPEG), to mimic the congested nature of the cellular environment (**Figure 5*a***) (52). In this study, k_{fold} greatly increased in the presence of hmwPEG. A scaled-particle theory for hard spheres (55, 56) can be used to provide estimates for the free energy change associated with a conformational equilibrium of an RNA in the presence of hmwPEG. Such a model assumes that hmwPEG molecules do not interact enthalpically with RNA and only exclude volume within the

solution. Temperature-dependent smFRET-based experiments can be exploited to provide direct experimental evidence for this assumption. The systematic crowding of RNA by hmwPEG has little to no effect on the enthalpic component of the folding free energy barrier, as indicated by nearly identical slopes in Eyring plots of the temperature-dependent rate constant data (**Figure 5*b*,*c***). Instead, the primary effect of hmwPEG is to entropically increase k_{fold}, as indicated by the systematic increase in the intercept of such a plot (**Figure 5*c***) (52). Thus, the observed molecular crowding effect appears to be almost completely entropic, which is consistent with the thermodynamic assumptions implicit in excluded volume models like scaled-particle theory. Importantly, without the additional support provided by these temperature-dependent smFRET experiments, one could have argued that the increased folding rate constant was the result of an enthalpically driven chemical interaction between hmwPEG and the RNA.

Additionally, our group has employed temperature-dependent smFRET techniques to probe the thermodynamic influence of osmolytes—highly soluble molecules that can be used to regulate the osmotic pressure within a cell [e.g., trimethylamine-*N*-oxide (TMAO) and urea]—on the equilibrium and kinetic properties of two different nucleic acid constructs (53): one designed to probe duplex hybridization (**Figure 3*a***) and the other containing the well-characterized GAAA tetraloop-tetraloop receptor interaction (**Figure 4*a***). Previous ensemble, equilibrium-based biophysical experiments had indicated that the conformational equilibria of nucleic acids (and proteins) are sensitive to the concentration of highly soluble cosolutes (**Figure 5*d***), with the degree of sensitivity largely determined by the amount of surface area buried during a structural rearrangement (57). However, little was known about how these osmolytes influence the kinetics and thermodynamics of nucleic acid conformational transitions. Fortunately, temperature-dependent smFRET techniques are perfect for exploring this topic. Accordingly, stage-based heating methods have been used in conjunction with smFRET to demonstrate that the well-documented destabilization of nucleic acids at elevated concentrations of urea (58) is largely a result of entropic considerations related to expulsion of this osmolyte from nucleobase surfaces during the formation of both secondary and tertiary structures (53). The entropic destabilization of the folding equilibrium occurs primarily via k_{unfold} in the case of DNA duplex association, whereas k_{fold} is more prominently influenced in the case of the GAAA tetraloop-tetraloop receptor interaction (**Figure 5*e*,*f***). Such observations highlight the important result that nucleobase surface burial occurs late (post-transition state) along the folding pathway for secondary structure formation and early (pre-transition state) along the folding pathway for tertiary structure formation.

In recent years, a few ensemble biophysical studies have revealed that various protein stabilizing agents, such as TMAO, can also stabilize higher-order structures in nucleic acids (**Figure 5*c***), again in a manner that depends on the amount of surface area buried during the conformational transition (59). In contrast to the predominantly entropic origin of urea-inhibited nucleic acid folding, TMAO-facilitated conformational transitions appear to be more variable, particularly regarding tertiary structure formation. Although TMAO slightly promotes secondary structure formation in DNA, purely by reducing the entropic cost of folding (53), the presence of this osmolyte can more efficiently stabilize RNA tertiary structures. This occurs via an increase in k_{fold}, resulting from a less endothermic free energy barrier that outweighs the more ordered free energy barrier (53) (**Figure 5*e***), with little to no effect on k_{unfold} (**Figure 5*f***). In general, these smFRET studies support the established notion that nucleic acid structure formation is facilitated by TMAO. However, the thermodynamically distinct behavior of secondary and tertiary structures reveals that the degree of stabilization is modulated by TMAO's unfavorable interactions with the various surfaces of nucleic acids that are buried during a folding transition, specifically weak, unfavorable interactions with nucleobase surfaces and strong, unfavorable, interactions with the phosphate surfaces. Importantly, the temperature-dependent smFRET component of this study

TEMPERATURE-DEPENDENT smFRET STUDIES OF PROTEINS

Although this review primarily highlights the use of temperature-dependent smFRET to advance our understanding of nucleic acid biophysics, it is worth mentioning that such techniques have also been used to facilitate our understanding of protein folding. In particular, a collection of temperature-dependent smFRET studies from the Schuler lab (22, 104, 105) have been used to clearly identify the thermodynamic origin of the well-documented temperature-dependent collapse of unfolded and unstructured proteins. Specifically, these studies revealed that hydrogen bonding interactions in the unfolded state and hydrophobic compaction are both responsible for the collapse of such unstructured proteins at elevated temperature (22). Additionally, these studies demonstrated that the same interactions are responsible for the expansion of cold-denatured proteins at lower temperatures (105). With the assistance of molecular dynamics simulations, these temperature-dependent smFRET studies revealed that, for hydrophilic peptides, the extent of collapse or expansion can be qualitatively described by a summation of the solvation energies of the constituent amino acids (104). In an important conclusion to this collection of protein folding studies conducted using temperature-dependent smFRET, these results can be reproduced in the context of live eukaryotic cells by using innovative techniques to perform such experiments in a cytosolic environment (106).

provides some of the first thermodynamic insights into osmolyte-influenced nucleic acid folding and helps build the foundation for future studies of nucleic acid conformational transitions in complex solutions akin to the cellular milieu.

As is apparent in the examples above, temperature-dependent smFRET-based experiments have proved to be a valuable tool for folding studies of all types of biopolymers. For instance, these methods have enabled qualitative exploration of the activation barriers associated with large conformational transitions in complex functional RNA; they have also allowed quantitative measurement of the entropic and enthalpic changes associated with transition state formation in isolated tertiary interactions. In all of the studies surveyed above, the thermodynamic and energetic insights afforded by temperature-dependent smFRET have (*a*) helped to enhance our understanding of the free energy landscape associated with these folding equilibria and (*b*) led to the development of structural and/or mechanistic models for these folding processes. Although not as abundant as their nucleic acid study counterparts, temperature-dependent smFRET studies of proteins have also unveiled important information about energetic landscapes and folding pathways (see the sidebar Temperature-Dependent smFRET Studies of Proteins). It is worth stressing that all of the biophysical insights obtained in these research efforts have been obtained using simple stage-based heating approaches. This collection of diverse temperature-dependent smFRET studies showcases temperature as an extremely valuable and relatively easy-to-control experimental parameter.

3. LASER-BASED HEATING

The feasibility and simplicity of stage-based heating techniques have allowed the smFRET community to make a diverse array of scientific discoveries. However, the technique itself is not without some drawbacks (60, 61). Some of the most important weaknesses arise because these devices slowly heat relatively large sample volumes. In typical stage-based heating techniques, great care should be taken to slowly warm and cool (1°C/min) the microscope objective, to avoid damaging it via rapid thermal expansion. This slow heating greatly limits experimentalists' ability to rapidly change the sample temperature in so-called single-molecule temperature-jump experiments. Another limitation is that most standard microscope objectives can only function properly

INDIRECT LASER-BASED HEATING OF smFRET SAMPLES

Recent experiments have demonstrated the feasibility of a similar approach to laser-based heating that uses laser light to indirectly modulate the temperature of fluorescent samples (107). Briefly, one can heat some thermally conductive material (typically a thin layer of metal) with focused laser light and then allow the warm metal surface to transfer thermal energy to the solution; thus, the laser light indirectly warms the sample. This technique has been used in conjunction with a cryostat to produce temperature changes of greater than 170 K in pure glycerol, with half-maximal heating times on the order of a few microseconds (108). These indirect laser-based heating methods have recently been used to perform so-called temperature-cycle experiments to help identify which physical parameters (e.g., dye orientation, dye photophysics, or polymer dynamics) give rise to heterogeneous E_{FRET} distributions for supposedly rigid biopolymers (109). The results of these experiments suggest that factors other than fluctuations in the end-to-end distance of the rigid polymers (e.g., linker dynamics and dye-dye or dye-polymer interactions) are most likely responsible for the unexpected E_{FRET} distributions, thus revealing some potential complications associated with biomolecular FRET.

at a relatively low temperature. Above 50°C, thermal expansion and softening of the index of refraction-matched optical adhesives can damage the precise alignment of optical elements within the objective, rendering it ineffective. Additionally, heating the entire solution can lead to more wide-spread sample degradation, which is especially problematic for complex macromolecular systems (e.g., ribosomes) and can lead to undesirable experimental artifacts.

To overcome these and other shortcomings associated with stage-based heating techniques, research efforts in our group have been directed toward heating volumes with physical dimensions significantly smaller than those of the entire sample. One particularly powerful and experimentally valuable approach with which to accomplish this task is to use focused laser light to heat a small volume within the sample. Generally, this can be accomplished with frequencies of infrared and near-infrared light that are resonant with the various vibrational bands of liquid water, whereby the laser light itself directly deposits thermal energy into the aqueous sample (for a discussion of techniques that use laser light to indirectly heat the sample solution, see the sidebar Indirect Laser-Based Heating of smFRET Samples). In this section, we explore (*a*) the more prominent technical aspects associated with direct laser-based heating approaches in smFRET experiments and (*b*) how the advantages of such techniques have allowed cleverly designed experiments to address thermally demanding problems related to nucleic acid folding.

3.1. Technical Details

For the past few decades, focused, high-energy, nanosecond pulses of near-infrared laser light have been used to temporarily and rapidly warm aqueous solutions, producing a so-called temperature jump (62), followed by a much slower return to ambient temperature. Various spectroscopies can be used to monitor the intrinsic fluorescence or ultraviolet absorbance of a biomolecular sample as it equilibrates to the elevated temperature generated by the infrared light. These ensemble temperature jump experiments provide experimental access to biomolecular dynamics occurring between the nanoseconds required to generate the maximum solution temperature and the milliseconds required for cooling. As always, the intrinsic complications associated with ensemble averaging can be avoided using single-molecule detection schemes. Accordingly, the basic principles behind these temperature-jump experiments (63–65) have recently been adapted to locally modulate the temperature of smFRET samples.

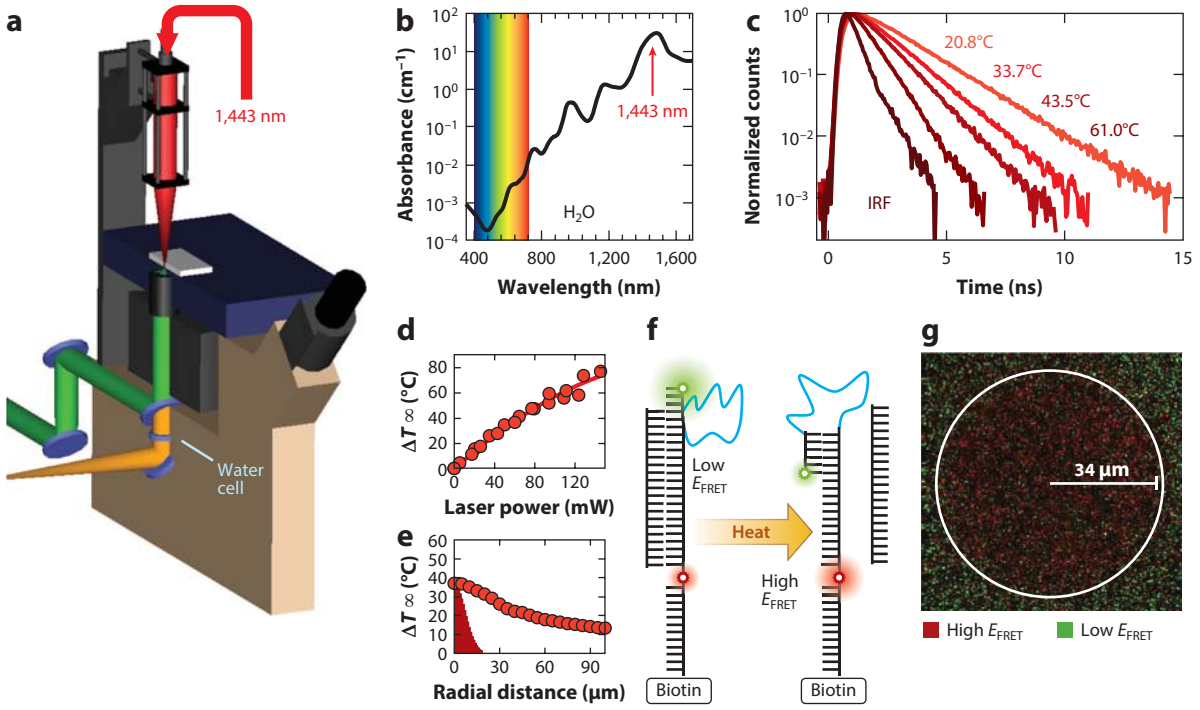

Figure 6

Laser-based heating techniques for smFRET. (*a*) Cutaway diagram of a confocal fluorescence microscope equipped with an infrared laser for heating applications. (*b*) Absorbance spectrum of water in the visible and infrared regions. Note the modest absorbance at 1,443 nm. (*c*) Temperature-dependent fluorescence decay of rhodamine B compared to the instrument response function (IRF), which limits the temporal resolution to a few hundred picoseconds. Fluorescence decay data acquired from picoliter volumes are fit to determine the fluorescence lifetime of rhodamine B, which is a function of the solution temperature. (*d*) Plot of steady-state temperature change versus incident infrared laser power. (*e*) Radial temperature profile associated with laser-based heating techniques. Notice how the temperature profile (*red circles*) is substantially broader than the profile of the infrared laser (*dark red histogram*). (*f*) Schematic representation of the 21-bp DNA duplex studied using pulsed infrared heating techniques. (*g*) Red-green, false-color surface representation of an area where the heating laser was used to promote the dissociation of a 21-bp DNA duplex. The circular region contains high-E_{FRET} molecules (*red*) that have undergone single dissociation events, whereas the outer region contains low-E_{FRET} (*green*) molecules that have resisted thermally induced dissociation. The data used to generate this figure were obtained from previously published smFRET efforts (60, 61) from our group.

A few different implementations and/or adaptations of these single-molecule temperature jumps have been described (61, 66–68). The most important aspect of such an experiment is, of course, a suitable source of near-infrared radiation, which is needed to heat the sample (**Figure 6*a***). Ideally, the wavelength of light should be resonant with, and modestly attenuated by, the molecular absorptions of water (62) (**Figure 6*b***), which correspond to frequencies associated with overtone and combination bands of the vibrational modes of liquid water near room temperature (69). These transiently excited vibrations quickly relax back down to a thermal distribution, depositing the excess absorbed energy into the solution and increasing its average kinetic energy (i.e., temperature) (70). Unlike many of the early ensemble temperature-jump experiments, which made use of nano- and picosecond pulsed lasers (62) with relatively high peak powers ($>10^6$ W), most smFRET laser-based heating methods use much lower-power (<1 W) continuous wave (cw) sources of infrared radiation. For a constant flux of photons, a simple physical model based on conservation

of energy suggests that the initial instantaneous heating rates ($[\partial T/\partial t]_{t=0}$) in aqueous solutions can exceed 10^6 °C/s, depending on (*a*) the infrared laser power (0.135 W) and wavelength (1,440–1,450 nm) of the heating laser and (*b*) the cross-sectional area (10^{-6} cm^2) of the approximately 10-pL heated volume (61). Furthermore, Newton's law of heating and cooling mandates that $[\partial T/\partial t]_{t=0}$ is linearly proportional to the asymptotic steady-state temperature change (ΔT_∞), which, for the parameters above, is measured to be roughly 80°C. The coefficient of proportionality relating these two quantities describes the exponential time constant associated with the heating process, $\tau_{heat} = \Delta T_\infty / [\partial T/\partial t]_{t=0}$ (i.e., the time required for the temperature to change by a factor of $1/e$), which, in the absence of any thermal diffusion, is approximately 10^{-4} s (61). Because both ΔT_∞ and $[\partial T/\partial t]_{t=0}$ scale approximately linearly with the incident laser power, τ_{heat} is largely independent of laser power (61). For the infrared cw lasers commonly used in smFRET experiments, the peak photon flux can easily be more than 10^6 times smaller than that of the pulsed sources used in ensemble temperature jumps, resulting in slower initial instantaneous heating rates. However, a cw heating source has the ability to achieve a steady-state temperature (albeit after $\approx 10^{-4}$ s) and indefinitely maintain that temperature until the heating laser is switched off. Conversely, for a low-repetition-rate, nanosecond-pulsed laser source, the packet of photons will pass through the sample very quickly, which limits the heating duration and allows the thermal bath to persist for only a few milliseconds before the sample cools to ambient temperature (62).

When operated as a continuous source of thermal control in smFRET experiments, the small heated volumes associated with laser-based heating alleviate several shortcomings traditionally associated with stage-based heating. First, because there is no need to regulate the temperature of the microscope objective, a need that previously restricted temperatures to <50°C, samples heated with laser-based techniques can routinely reach the boiling point of water (61, 66, 68). Second, the small heated volumes result in rapid ($\tau_{heat} < 10^{-3}$ s) sample heating that outperforms stage-based methods ($\tau_{heat} > 10^2$ s) by five orders of magnitude. Finally, thermally induced degradation of biological samples only occurs in picoliter heated volumes, which can be 10^6 times smaller than the microliter heated volumes typically associated with stage-based techniques.

To be able to observe and detect single-molecule fluorescence while heating, it is important to ensure that the detectors (e.g., single photon avalanche diodes) are not exposed to the comparably large photon count rates associated with >10 mW of infrared radiation. One relatively simple way to accomplish this task is to place a thin (e.g., 3-mm) water cell in the detection path (60) (**Figure 6*a***). Water is highly transparent with respect to visible electromagnetic radiation (transmission ≈ 1) and will not interfere with detection of the fluorescent photons. However it absorbs quite strongly at the wavelength of the heating laser (transmission $<10^{-8}$) (60), thus preventing unwanted excess infrared photons from reaching the detectors (**Figure 6*b***). Another challenge associated with picoliter heated volumes is the difficulty of accurately and reliably determining the sample temperature. To this end, the temperature-dependent fluorescence of rhodamine B (71) (**Figure 6*c***) can be used to generate a calibration curve, using, for example, an Eyring analysis of the temperature-dependent nonradiative component of the fluorescent lifetime (60), although microscopic thermocouples (66) and quantum dots (72) represent other possible means for micrometer-scale temperature determination.

As a preliminary validation of the method and all of the associated technical aspects, a heating-while-observing laser-based heating technique has been used to measure the temperature-dependent folding kinetics of the GAAA tetraloop-tetraloop receptor tertiary interaction (60) in a way that is nearly identical to what has been done previously using stage-based heating methods (21). Reassuringly, the two techniques produce results that are experimentally indistinguishable. Not only do these results demonstrate that laser-based approaches can be as accurate and reliable

as stage-based methods, they also reveal the feasibility of performing temperature-dependent smFRET experiments with laser-based temperature control.

As a follow up on this preliminary study, additional efforts have produced a quantitative characterization of the thermal (**Figure 6*d***), spatial (**Figure 6*e***), and temporal properties (61) of such a direct infrared-based heating system using the fluorescence lifetime of rhodamine B as a measure of the solution temperature. This endeavor highlights three important advantages of laser-based heating: (*a*) the time scales for the heating process are faster than a millisecond, (*b*) the heated volumes are quite small (10^{-12} L), and (*c*) the maximum temperature change is rather large (>80°C). Additionally, this investigation has revealed that complex fluid dynamics related to thermal diffusion and convective processes may influence the spatial, temporal, and thermal characteristics of the heated volumes. Specifically, the expected linear dependence of ΔT_∞ on laser power begins to break down at high laser power (**Figure 6*d***), the steady-state radial temperature profile [**Figure 6*e***; full width at half maximum (FWHM) >100 μm] is always substantially broader than the infrared beam itself (FWHM = 17 μm), and the time constants for heating and cooling are only comparable for short heating durations (61). These observations all point toward a subtle but important contribution of fluid dynamics to the spatial, temporal, and thermal properties of laser-based heating in smFRET experiments.

3.2. smFRET Temperature Jumps

Despite the subtle complexities associated with fluid dynamics, direct laser-based heating remains an accurate, reliable, and versatile way to rapidly modulate the sample temperature in smFRET experiments, particularly after thorough and rigorous characterization. This versatility can be easily exploited to quickly adjust the power output of the infrared laser as a function of time, which provides the ability to rapidly cycle between desired steady-state temperatures. The pulses of heat associated with rapid temperature cycling can be used to thermally promote various activated biochemical processes of interest in a fashion similar to the ensemble temperature-jump experiments mentioned at the beginning of Section 3.

Such laser-based heating approaches are relatively unexplored and have thus far only been applied to a handful of biophysical problems, perhaps the most conceptually simple being the thermally induced dissociation of highly stable duplex nucleic acids. These experiments make use of laser-based heating methods designed for either confocal or TIRF microscopes (61, 66, 67). Initially, such duplex dissociation experiments were used to demonstrate the applicability of laser-based temperature jumps in TIRF-based smFRET experiments (66, 67), and a short time later they were applied to a confocal smFRET microscope to more rigorously and quantitatively explore the kinetics and thermodynamics of this ubiquitous biological process (61). In these experiments, DNA constructs containing a 21-bp duplex were immobilized to a microscope coverslip (**Figure 6*f***). One strand of the duplex contained both the biotin (for immobilization) and the Cy3-Cy5 donor-acceptor FRET pair, such that in the duplex conformation, the nonmodified complementary strand would ensure that the two fluorophores were sufficiently separated, resulting in minimal energy transfer from the donor to the acceptor. After thermally induced dissociation of the complementary strand, the remaining surface-immobilized strand was designed to rapidly refold into a loop-like structure, greatly increasing the proximity of the donor-acceptor pair and thereby greatly enhancing the E_{FRET}.

This 21-bp DNA duplex (**Figure 6*f***) is sufficiently stable, such that at room temperature it will not dissociate, even after hundreds of minutes. Importantly, substantial dissociation is only observed after exposure to high intensity infrared light (**Figure 6*g***), where each heating event can be described by its duration, Δt, and its steady state temperature change, ΔT_∞. The time- and

temperature-dependent probability of resisting dissociation, referred to as the survival probability, is a function of these two properties [i.e., $P_{\text{survival}}(\Delta T_\infty, \Delta t)$]. Pulsed heating experiments, which systematically vary both ΔT_∞ and Δt, reveal that the survival probability of a 21-bp DNA duplex decreases more slowly at short heating than at long heating times. This results in a temporal lag between the start of the heating pulse and the complete dissociation of the DNA duplex. Such temporal lag is an observation commonly associated with a consecutive multistep kinetic process depicted in the model below:

$$A_0 \xrightarrow{K_{01}(\Delta T_\infty)} A_1 \cdots \xrightarrow{K_{1n}(\Delta T_\infty)} A_n \xrightarrow{K_{nB}(\Delta T_\infty)} B. \tag{5}$$

Such processes have previously been used to describe the biochemical activity of various helicases (73, 74), which function to enzymatically dissociate duplex DNA.

Provided that all of the n consecutive rate constants in the above model are identical to a common rate constant [i.e., $k(\Delta T_\infty)$], an exact solution for the survival probability exists and can be represented by a ratio of Γ functions (Equation 6):

$$P_{\text{survival}}(\Delta T_\infty, \Delta t) = \frac{\Gamma\left(n, k(\Delta T_\infty), \Delta t\right)}{\Gamma(n)}. \tag{6}$$

A global analysis of the survival probability data reveals that four consecutive kinetic steps best describe the dissociation kinetics of the 21-bp DNA duplex. The temperature dependence of this consecutive rate constant [i.e., $k(\Delta T_\infty)$] suggests the presence of a free energy barrier with strong enthalpic [$\Delta H^\ddagger = 50(10)$ kcal/mol] and entropic [$\Delta S^\ddagger = 100(20)$ cal/(mol · K)] components. This information has been used to develop physical insights into this highly consecutive process. Specifically, these thermodynamic parameters correspond to the standard-state enthalpy changes associated with breaking between ≈6 DNA base pairs and the entropy changes associated with breaking between ≈4.5 base pairs. Interestingly, four consecutive events of this nature nicely predict the complete dissociation of the 21-bp DNA duplex. These consecutive processes are attributed to thermally activated fraying events at both ends of DNA duplexes, which must occur prior to rapid dissociation. Such a model proposes that when a long (>20-bp) DNA duplex melts, it does so from both ends, until a sufficiently small number of base pairs remain in the middle of the complex, at which point the two strands dissociate, completing the melting process.

4. EXPERIMENTAL CHALLENGES

Although the past 10 years have witnessed a rapid evolution in ways to provide temperature control in smFRET experiments [e.g., microfluidics (46, 75) and laser-based heating (60, 66)], experimental challenges remain, particularly at temperatures above 50°C. Arguably one of the most pressing issues associated with temperature-dependent smFRET studies is the lack of thermally stable fluorophores. Most commonly used organic dyes have temperature-dependent quantum yields (76, 77), with Cy3 and Cy5 being among the worst performers in terms of reduced photon yields at elevated temperatures. In most cases, this process probably results from preferential thermal activation of nonradiative relaxation pathways, which outcompete the desired radiative relaxation. In the case of rhodamine B, such temperature-dependent fluorescence has fortuitously been exploited as a fluorogenic temperature sensor. Nevertheless, this phenomenon routinely prevents adequate photon collection from single fluorophores at temperatures higher than 50°C, making it difficult to simultaneously heat and observe thermally stable biomolecular folding processes. Additionally, temperature can differentially alter the detection efficiencies of such fluorophores, which will introduce errors into absolute distance calculations via FRET if these alterations are not properly taken into consideration.

Because single-molecule data quality increases with the number of photons collected, research efforts have identified numerous ways to increase maximum attainable photon count rates. These methods could potentially be used to circumvent the problems associated with temperature-dependent fluorophores. Initially, efforts were directed at identifying photoprotection cocktails consisting of oxygen scavengers and antioxidants to enhance the photostability of common organic fluorophores (78–82). More recently, attempts have been made to covalently couple these photoprotection agents to fluorophores, which seems to enhance their performance (83–86). Additionally, rigid fluorophores have been developed that are less susceptible to thermally promoted nonradiative relaxation (87). Many of these fluorophore-based approaches may prove to be useful in future smFRET studies at elevated temperatures. Alternatively, researchers have tried to exploit the physical and optical properties of various materials to enhance the excitation and detection efficiencies of various single-molecule fluorescence experiments. Such trials have led to the development and implementation of micro- and nanoscopic devices, such as zero-mode wave guides (88, 89), small metal nanostructures (90–92), and colloidal lenses (93). The enhancements afforded by these methodologies could also be useful for temperature-dependent smFRET measurements suffering from low photon outputs.

Another consideration to take into account for applications requiring local heating of small experimental volumes (e.g., laser-based heating) is thermophoresis (94). The existence of any strong temperature gradients will result in the directed motion of molecules, depending on their solvation entropies (94). Although the effects of thermophoresis have recently been exploited to measure conformational changes of biomolecules (95), this interesting physical phenomenon substantially impairs researchers' ability to study freely diffusing single molecules in a confocal microscope system, because it will often depopulate the heated detection volume of fluorescent particles. Nevertheless, these laser-based heating approaches have been used in conjunction with ensemble FRET methods to study the folding stability and dynamics of proteins in live cells (96) and of DNA hairpins in a microfluidic device (97). To sidestep the intrinsic challenges associated with thermophoresis, most laser-based heating techniques probe surface-immobilized molecules. However, many of the commonly employed surface immobilization practices make use of noncovalent ligand-protein interactions, like that of biotin-streptavidin (12). Of course, dissociation of this noncovalent interaction is also a thermally activated process (98). Fortunately, at room temperature the dissociation rate constant ($k_{diss} \approx 10^{-6}$ s^{-1}) of biotin from streptavidin (99) is orders of magnitude slower than the reciprocal of most immobilized smFRET observation times (typically $\approx 10^1$–10^3 s), rendering surface detachment a negligible factor. However, at even moderately elevated temperatures, this process is greatly accelerated, resulting in dissociation rate constants in excess of 10^{-1} s^{-1} (98). Fortunately, great efforts have been made to exploit various covalent chemistries to aid in developing surface immobilization strategies (100, 101) that should be significantly more resistant to temperature. In conjunction with strategies to increase photon count rates, immobilization strategies will greatly facilitate high-temperature observation time in surface-immobilized smFRET experiments.

5. FINAL THOUGHTS

Over the past few decades, smFRET has been an extremely important biophysical tool that has routinely been used to conduct studies of biomolecular folding. Every so often, this powerful technique is coupled with thermal control to partition free energies associated with rate and equilibrium constants into their enthalpic and entropic components. Successful completion of this task provides access to valuable thermodynamic information from single-molecule studies,

as highlighted in this review. Specifically, such temperature-dependent smFRET studies have helped to (*a*) verify the mechanistic details related to the association and dissociation of two complementary oligonucleotides, (*b*) elucidate the entropic and enthalpic contributions to the free energy landscape of multiple structured RNAs, and (*c*) unveil the thermodynamic origins of various cosolute (e.g., salt, osmolyte, and crowding agent) influenced conformational transitions in nucleic acids. Regardless of how temperature is controlled in a particular smFRET experiment, its use as an additional experimental parameter has provided an enhanced thermodynamic understanding of several biophysical problems covering a diverse collection of research topics. However, a nearly limitless supply of unanswered questions that are amenable to such techniques still exists. Thus it remains clear that, as the biophysical community continues to refine its understanding of free energy landscapes, temperature-dependent smFRET experiments will continue to be an extremely rich source of detailed thermodynamic information.

SUMMARY POINTS

1. Stage-based sample heating approaches can readily be applied to any smFRET microscope, making them a popular choice for temperature-dependent folding studies of proteins, nucleic acids, and other biomolecules.
2. Temperature-dependent smFRET experiments have been used to partition biomolecular free energy landscapes into their enthalpic and entropic components, providing access to valuable thermodynamic details about the associated equilibrium processes.
3. Although it is easy to use, and therefore commonly implemented, stage-based heating has significant experimental limitations. Fortunately, these limitations can be partially avoided by using laser-based heating.
4. Versatile laser-based heating approaches enable rapid modulation of sample temperatures (e.g., temperature jumps, pulses, and cycles) and can be used to thermally activate otherwise slow biological processes.
5. Laser-based heating approaches also have temperature-dependent constraints related to fluorescence quantum yields, surface dissociation, and thermophoresis, which can potentially be overcome using various experimental adaptations.
6. Despite the apparent challenges, numerous biophysical advances have been achieved using temperature-dependent smFRET, and such advances will continue to help refine our understanding of biomolecular free energy landscapes.

DISCLOSURE STATEMENT

The authors are not aware of any affiliations, memberships, funding, or financial holdings that might be perceived as affecting the objectivity of this review.

ACKNOWLEDGMENTS

We gratefully acknowledge support for this work from the National Science Foundation (CHE 1266416, PHY 1125844), with additional equipment funds for early development of the smFRET apparatus coming from the National Institute of Standards and Technology.

LITERATURE CITED

1. Orrit M, Bernard J. 1990. Single pentacene molecules detected by fluorescence excitation in a *p*-terphenyl crystal. *Phys. Rev. Lett.* 65:2716–19
2. Moerner WE, Kador L. 1989. Optical detection and spectroscopy of single molecules in a solid. *Phys. Rev. Lett.* 62:2535–38
3. Orrit M. 2015. Single-molecule chemistry is more than superresolved fluorescence microscopy. *Angew. Chem. Int. Ed.* 54:8004–5
4. Moerner WE, Orrit M. 1999. Illuminating single molecules in condensed matter. *Science* 283:1670–76
5. Forster T. 1948. Zwischenmolekulare energiewanderung und fluoreszenz. *Ann. Phys.* 2:55–75
6. Ha T, Enderle T, Ogletree DF, Chemla DS, Selvin PR, Weiss S. 1996. Probing the interaction between two single molecules: fluorescence resonance energy transfer between a single donor and a single acceptor. *PNAS* 93:6264–68
7. Stryer L. 1978. Fluorescence energy transfer as a spectroscopic ruler. *Annu. Rev. Biochem.* 47:819–46
8. Stryer L, Haugland RP. 1967. Energy transfer: a spectroscopic ruler. *PNAS* 58:719–26
9. Deniz AA, Laurence TA, Dahan M, Chemla DS, Schultz PG, Weiss S. 2001. Ratiometric single-molecule studies of freely diffusing biomolecules. *Annu. Rev. Phys. Chem.* 52:233–53
10. Ha T. 2001. Single-molecule fluorescence resonance energy transfer. *Methods* 25:78–86
11. Weiss S. 1999. Fluorescence spectroscopy of single biomolecules. *Science* 283:1676–83
12. Roy R, Hohng S, Ha T. 2008. A practical guide to single-molecule FRET. *Nat. Methods* 5:507–16
13. Joo C, Balci H, Ishitsuka Y, Buranachai C, Ha T. 2008. Advances in single-molecule fluorescence methods for molecular biology. *Annu. Rev. Biochem.* 77:51–76
14. Okamoto K. 2013. Introduction of FRET application to biological single-molecule experiments. *Int. J. Biophys.* 3:9–17
15. Borgia A, Williams PM, Clarke J. 2008. Single-molecule studies of protein folding. *Annu. Rev. Biochem.* 77:101–25
16. Schuler B. 2013. Single-molecule FRET of protein structure and dynamics—a primer. *J. Nanobiotechnol.* 11(Suppl. 1):S2
17. Schuler B, Hofmann H. 2013. Single-molecule spectroscopy of protein folding dynamics—expanding scope and timescales. *Curr. Opin. Struct. Biol.* 23:36–47
18. Chung HS, Gopich IV. 2014. Fast single-molecule FRET spectroscopy: theory and experiment. *Phys. Chem. Chem. Phys.* 16:18644–57
19. Banerjee PR, Deniz AA. 2014. Shedding light on protein folding landscapes by single-molecule fluorescence. *Chem. Soc. Rev.* 43:1172–88
20. Benedikt K, Koberling F, Fiore JL. 2008. *Technical Note: Sample Temperature Control for Single Molecule Experiments with the MicroTime 200*. Berlin: PicoQuant
21. Fiore JL, Kraemer B, Koberling F, Edmann R, Nesbitt DJ. 2009. Enthalpy-driven RNA folding: single-molecule thermodynamics of tetraloop-receptor tertiary interaction. *Biochemistry* 48:2550–58
22. Nettels D, Muller-Spath S, Kuster F, Hofmann H, Haenni D, et al. 2009. Single-molecule spectroscopy of the temperature-induced collapse of unfolded proteins. *PNAS* 106:20740–45
23. Le TT, Kim HD. 2014. Studying DNA looping by single-molecule FRET. *J. Vis. Exp.* 88:e51667
24. Zhao R, Rueda D. 2009. RNA folding dynamics by single-molecule fluorescence resonance energy transfer. *Methods* 49:112–17
25. Shaw E, St-Pierre P, McCluskey K, Lafontaine DA, Penedo JC. 2014. Using sm-FRET and denaturants to reveal folding landscapes. *Methods Enzymol.* 549:313–41
26. Hodak JH, Fiore JL, Nesbitt DJ, Downey CD, Pardi A. 2005. Docking kinetics and equilibrium of a GAAA tetraloop-receptor motif probed by single-molecule FRET. *PNAS* 102:10505–10
27. Blanco M, Walter NG. 2010. Analysis of complex single-molecule FRET time trajectories. *Methods Enzymol.* 472:153–78
28. McKinney SA, Joo C, Ha T. 2006. Analysis of single-molecule FRET trajectories using hidden Markov modeling. *Biophys. J.* 91:1941–51
29. Nicolai C, Sachs F. 2013. Solving ion channel kinetics with the QuB software. *Biophys. Rev. Lett.* 8:191–211

30. Bronson JE, Fei J, Hofman JM, Gonzalez RL Jr., Wiggins CH. 2009. Learning rates and states from biophysical time series: a Bayesian approach to model selection and single-molecule FRET data. *Biophys. J.* 97:3196–205
31. Holmstrom ED, Fiore JL, Nesbitt DJ. 2012. Thermodynamic origins of monovalent facilitated RNA folding. *Biochemistry* 51:3732–43
32. Rice SA, Doty P. 1957. The thermal denaturation of desoxyribose nucleic acid. *J. Am. Chem. Soc.* 79:3937–47
33. Puglisi JD, Tinoco I Jr. 1989. Absorbance melting curves of RNA. *Methods Enzymol.* 180:304–25
34. Marky LA, Breslauer KJ. 1987. Calculating thermodynamic data for transitions of any molecularity from equilibrium melting curves. *Biopolymers* 26:1601–20
35. SantaLucia J Jr., Hicks D. 2004. The thermodynamics of DNA structural motifs. *Annu. Rev. Biophys. Biomol. Struct.* 33:415–40
36. Varani G. 1995. Exceptionally stable nucleic acid hairpins. *Annu. Rev. Biophys. Biomol. Struct.* 24:379–404
37. Mergny JL, Lacroix L. 2003. Analysis of thermal melting curves. *Oligonucleotides* 13:515–37
38. Turner DH, Mathews DH. 2010. NNDB: the nearest neighbor parameter database for predicting stability of nucleic acid secondary structure. *Nucleic Acids Res.* 38:D280–82
39. Mathews DH, Moss WN, Turner DH. 2010. Folding and finding RNA secondary structure. *Cold Spring Harb. Perspect. Biol.* 2:a003665
40. Zuker M. 2003. Mfold web server for nucleic acid folding and hybridization prediction. *Nucleic Acids Res.* 31:3406–15
41. Grunwell JR, Glass JL, Lacoste TD, Deniz AA, Chemla DS, Schultz PG. 2001. Monitoring the conformational fluctuations of DNA hairpins using single-pair fluorescence resonance energy transfer. *J. Am. Chem. Soc.* 123:4295–303
42. Dupuis NF, Holmstrom ED, Nesbitt DJ. 2013. Single-molecule kinetics reveal cation-promoted DNA duplex formation through ordering of single-stranded helices. *Biophys. J.* 105:756–66
43. Ying L, Green JJ, Li H, Klenerman D, Balasubramanian S. 2003. Studies on the structure and dynamics of the human telomeric G quadruplex by single-molecule fluorescence resonance energy transfer. *PNAS* 100:14629–34
44. Bartley LE, Zhuang XW, Das R, Chu S, Herschlag D. 2003. Exploration of the transition state for tertiary structure formation between an RNA helix and a large structured RNA. *J. Mol. Biol.* 328:1011–26
45. Hohng S, Wilson TJ, Tan E, Clegg RM, Lilley DMJ, Ha TJ. 2004. Conformational flexibility of four-way junctions in RNA. *J. Mol. Biol.* 336:69–79
46. Wang B, Ho J, Fei J, Gonzalez RL Jr., Lin Q. 2011. A microfluidic approach for investigating the temperature dependence of biomolecular activity with single-molecule resolution. *Lab. Chip* 11:274–81
47. Vesnaver G, Breslauer KJ. 1991. The contribution of DNA single-stranded order to the thermodynamics of duplex formation. *PNAS* 88:3569–73
48. Fiore JL, Nesbitt DJ. 2013. An RNA folding motif: GNRA tetraloop-receptor interactions. *Q. Rev. Biophys.* 46:223–64
49. Fiore JL, Holmstrom ED, Nesbitt DJ. 2012. Entropic origin of Mg^{2+}-facilitated RNA folding. *PNAS* 109:2902–7
50. Silverman SK, Cech TR. 2001. An early transition state for folding of the P4–P6 RNA domain. *RNA* 7:161–66
51. Bokinsky G, Rueda D, Misra VK, Rhodes MM, Gordus A, et al. 2003. Single-molecule transition-state analysis of RNA folding. *PNAS* 100:9302–7
52. Dupuis NF, Holmstrom ED, Nesbitt DJ. 2014. Molecular-crowding effects on single-molecule RNA folding/unfolding thermodynamics and kinetics. *PNAS* 111:8464–69
53. Holmstrom ED, Dupuis NF, Nesbitt DJ. 2015. Kinetic and thermodynamic origins of osmolyte-influenced nucleic acid folding. *J. Phys. Chem. B* 119:3687–96
54. Fulton AB. 1982. How crowded is the cytoplasm? *Cell* 30:345–47
55. Reiss H, Frisch HL, Lebowitz JL. 1959. Statistical mechanics of rigid spheres. *J. Chem. Phys.* 31:369–80
56. Lebowitz JL, Helfand E, Praestga E. 1965. Scaled particle theory of fluid mixtures. *J. Chem. Phys.* 43:774–79

57. Lambert D, Leipply D, Draper DE. 2010. The osmolyte TMAO stabilizes native RNA tertiary structures in the absence of Mg^{2+}: evidence for a large barrier to folding from phosphate dehydration. *J. Mol. Biol.* 404:138–57
58. Shelton VM, Sosnick TR, Pan T. 1999. Applicability of urea in the thermodynamic analysis of secondary and tertiary RNA folding. *Biochemistry* 38:16831–39
59. Lambert D, Draper DE. 2012. Denaturation of RNA secondary and tertiary structure by urea: Simple unfolded state models and free energy parameters account for measured m-values. *Biochemistry* 51:9014–26
60. Holmstrom ED, Nesbitt DJ. 2010. Real-time infrared overtone laser control of temperature in picoliter H_2O samples: "nanobathtubs" for single molecule microscopy. *J. Phys. Chem. Lett.* 1:2264–68
61. Holmstrom ED, Dupuis NF, Nesbitt DJ. 2014. Pulsed IR heating studies of single-molecule DNA duplex dissociation kinetics and thermodynamics. *Biophys. J.* 106:220–31
62. Kubelka J. 2009. Time-resolved methods in biophysics. 9. Laser temperature-jump methods for investigating biomolecular dynamics. *Photochem. Photobiol. Sci.* 8:499–512
63. Nelson JW, Tinoco I Jr. 1982. Comparison of the kinetics of ribooligonucleotide, deoxyribooligonucleotide, and hybrid oligonucleotide double-strand formation by temperature-jump kinetics. *Biochemistry* 21:5289–95
64. Gruebele M, Sabelko J, Ballew R, Ervin J. 1998. Laser temperature jump induced protein refolding. *Acc. Chem. Res.* 31:699–707
65. Thompson PA, Eaton WA, Hofrichter J. 1997. Laser temperature jump study of the helix $\rightleftharpoons$ coil kinetics of an alanine peptide interpreted with a 'kinetic zipper' model. *Biochemistry* 36:9200–10
66. Zhao R, Marshall M, Aleman EA, Lamichhane R, Feig A, Rueda D. 2010. Laser-assisted single-molecule refolding (LASR). *Biophys. J.* 99:1925–31
67. Paudel B, Rueda D. 2014. RNA folding dynamics using laser-assisted single-molecule refolding. *Methods Mol. Biol.* 1086:289–307
68. Hung MS, Kurosawa O, Washizu M. 2012. Single DNA molecule denaturation using laser-induced heating. *Mol. Cell Probe* 26:107–12
69. Curcio JA, Petty CC. 1951. The near infrared absorption spectrum of liquid water. *J. Opt. Soc. Am.* 41:302–4
70. Phillips CM, Mizutani Y, Hochstrasser RM. 1995. Ultrafast thermally induced unfolding of RNase A. *PNAS* 92:7292–96
71. Karstens T, Kobs K. 1980. Rhodamine B and rhodamine 101 as reference substances for fluorescence quantum yield measurements. *J. Phys. Chem.* 84:1871–72
72. Li S, Zhang K, Yang JM, Lin LW, Yang H. 2007. Single quantum dots as local temperature markers. *Nano Lett.* 7:3102–5
73. Park J, Myong S, Niedziela-Majka A, Lee KS, Yu J, et al. 2010. PcrA helicase dismantles RecA filaments by reeling in DNA in uniform steps. *Cell* 142:544–55
74. Ragunathan K, Joo C, Ha T. 2011. Real-time observation of strand exchange reaction with high spatiotemporal resolution. *Structure* 19:1064–73
75. Wunderlich B, Nettels D, Benke S, Clark J, Weidner S, et al. 2013. Microfluidic mixer designed for performing single-molecule kinetics with confocal detection on timescales from milliseconds to minutes. *Nat. Protoc.* 8:1459–74
76. Sanborn ME, Connolly BK, Gurunathan K, Levitus M. 2007. Fluorescence properties and photophysics of the sulfoindocyanine Cy3 linked covalently to DNA. *J. Phys. Chem. B* 111:11064–74
77. You Y, Tataurov AV, Owczarzy R. 2011. Measuring thermodynamic details of DNA hybridization using fluorescence. *Biopolymers* 95:472–86
78. Ha T, Tinnefeld P. 2012. Photophysics of fluorescent probes for single-molecule biophysics and super-resolution imaging. *Annu. Rev. Phys. Chem.* 63:595–617
79. Aitken CE, Marshall RA, Puglisi JD. 2008. An oxygen scavenging system for improvement of dye stability in single-molecule fluorescence experiments. *Biophys. J.* 94:1826–35
80. Zheng Q, Juette MF, Jockusch S, Wasserman MR, Zhou Z, et al. 2014. Ultra-stable organic fluorophores for single-molecule research. *Chem. Soc. Rev.* 43:1044–56

81. Swoboda M, Henig J, Cheng HM, Brugger D, Haltrich D, et al. 2012. Enzymatic oxygen scavenging for photostability without pH drop in single-molecule experiments. *ACS Nano* 6:6364–69
82. Dave R, Terry DS, Munro JB, Blanchard SC. 2009. Mitigating unwanted photophysical processes for improved single-molecule fluorescence imaging. *Biophys. J.* 96:2371–81
83. Blanchard SC. 2012. 'Self-healing' dyes: intramolecular stabilization of organic fluorophores reply. *Nat. Methods* 9:427–28
84. Tinnefeld P, Cordes T. 2012. 'Self-healing' dyes: intramolecular stabilization of organic fluorophores. *Nat. Methods* 9:426–27
85. Altman RB, Zheng Q, Zhou Z, Terry DS, Warren JD, Blanchard SC. 2012. Enhanced photostability of cyanine fluorophores across the visible spectrum. *Nat. Methods* 9:428–29
86. van der Velde JHM, Oelerich J, Huang J, Smit JH, Aminian Jazi A, et al. 2016. A simple and versatile design concept for fluorophore derivatives with intramolecular photostabilization. *Nat. Commun.* 7:10144
87. Cooper M, Ebner A, Briggs M, Burrows M, Gardner N, et al. 2004. Cy3B^{TM}: improving the performance of cyanine dyes. *J. Fluoresc.* 14:145–50
88. Levene MJ, Korlach J, Turner SW, Foquet M, Craighead HG, Webb WW. 2003. Zero-mode waveguides for single-molecule analysis at high concentrations. *Science* 299:682–86
89. Zhu P, Craighead HG. 2012. Zero-mode waveguides for single-molecule analysis. *Annu. Rev. Biophys.* 41:269–93
90. Langguth L, Punj D, Wenger J, Koenderink AF. 2013. Plasmonic band structure controls single-molecule fluorescence. *ACS Nano* 7:8840–48
91. Punj D, de Torres J, Rigneault H, Wenger J. 2013. Gold nanoparticles for enhanced single molecule fluorescence analysis at micromolar concentration. *Opt. Express* 21:27338–43
92. Punj D, Mivelle M, Moparthi SB, van Zanten TS, Rigneault H, et al. 2013. A plasmonic 'antenna-in-box' platform for enhanced single-molecule analysis at micromolar concentrations. *Nat. Nanotechnol.* 8:512–16
93. Schwartz JJ, Stavrakis S, Quake SR. 2010. Colloidal lenses allow high-temperature single-molecule imaging and improve fluorophore photostability. *Nat. Nanotechnol.* 5:127–32
94. Duhr S, Braun D. 2006. Why molecules move along a temperature gradient. *PNAS* 103:19678–82
95. Jerabek-Willemsen M, Wienken CJ, Braun D, Baaske P, Duhr S. 2011. Molecular interaction studies using microscale thermophoresis. *Assay Drug Dev. Technol.* 9:342–53
96. Ebbinghaus S, Dhar A, McDonald JD, Gruebele M. 2010. Protein folding stability and dynamics imaged in a living cell. *Nat. Methods* 7:319–23
97. Polinkovsky ME, Gambin Y, Banerjee PR, Erickstad MJ, Groisman A, Deniz AA. 2014. Ultrafast cooling reveals microsecond-scale biomolecular dynamics. *Nat. Commun.* 5:5737
98. Holmberg A, Blomstergren A, Nord O, Lukacs M, Lundeberg J, Uhlen M. 2005. The biotin-streptavidin interaction can be reversibly broken using water at elevated temperatures. *Electrophoresis* 26:501–10
99. Hyre DE, Le Trong I, Merritt EA, Eccleston JF, Green NM, et al. 2006. Cooperative hydrogen bond interactions in the streptavidin-biotin system. *Protein Sci* 15:459–67
100. Janissen R, Oberbarnscheidt L, Oesterhelt F. 2009. Optimized straight forward procedure for covalent surface immobilization of different biomolecules for single molecule applications. *Colloid Surf. B* 71:200–7
101. Aleman EA, Pedini HS, Rueda D. 2009. Covalent-bond-based immobilization approaches for single-molecule fluorescence. *ChemBioChem* 10:2862–66
102. Wang B, Fei JY, Gonzalez RL, Lin Q. 2007. *Single-molecule detection in temperature-controlled microchannels*. Presented at 2nd IEEE Int. Conf. Nano/Micro Eng. Mol. Syst., Jan. 16–19, Bangkok
103. Chen J, Dalal RV, Petrov AN, Tsai A, O'Leary SE, et al. 2014. High-throughput platform for real-time monitoring of biological processes by multicolor single-molecule fluorescence. *PNAS* 111:664–69
104. Wuttke R, Hofmann H, Nettels D, Borgia MB, Mittal J, et al. 2014. Temperature-dependent solvation modulates the dimensions of disordered proteins. *PNAS* 111:5213–18
105. Aznauryan M, Nettels D, Holla A, Hofmann H, Schuler B. 2013. Single-molecule spectroscopy of cold denaturation and the temperature-induced collapse of unfolded proteins. *J. Am. Chem. Soc.* 135:14040–43
106. Konig I, Zarrine-Afsar A, Aznauryan M, Soranno A, Wunderlich B, et al. 2015. Single-molecule spectroscopy of protein conformational dynamics in live eukaryotic cells. *Nat. Meth.* 12:773–79

107. Yuan H, Xia T, Schuler B, Orrit M. 2011. Temperature-cycle single-molecule FRET microscopy on polyprolines. *Phys. Chem. Chem. Phys.* 13:1762–69
108. Zondervan R, Kulzer F, van der Meer H, Disselhorst JA, Orrit M. 2006. Laser-driven microsecond temperature cycles analyzed by fluorescence polarization microscopy. *Biophys. J.* 90:2958–69
109. Yuan H, Gaiduk A, Siekierzycka JR, Fujiyoshi S, Matsushita M, et al. 2015. Temperature-cycle microscopy reveals single-molecule conformational heterogeneity. *Phys. Chem. Chem. Phys.* 17:6532–44

Annual Review of
Physical Chemistry
Volume 67, 2016

Contents

Indexes

Errata

An online log of corrections to *Annual Review of Physical Chemistry* articles may be found at http://www.annualreviews.org/errata/physchem